Lab 2 - EMG Measurement and Processing

Introduction

In this lab, EMG data was recorded from the forearm and biceps for two different experiments. The first experiment observed the biceps during elbow flexions to understand filtering techniques in MATLAB. The second experiment observed the forearm fist clenches to activate an Arduino connected servo motor using sample code provided.

Methods

The first half of the lab procedure required us to examine EMG data from the bicep muscle during elbow flexion. This required the usage of a device called a BioRadio, which can connect to a computer through Bluetooth using the BioCapture software to communicate the data. For the BioRadio to record EMG data, three electrodes had to be connected to the arm, two on the bicep for the differential channel and one on the elbow for the ground.

The placement of electrodes for this experiment was very important. The two surface electrodes on the bicep need to be fairly close together in order to prevent cross EMG readings from adjacent muscles. (1) The placement of the ground electrode is especially important, as it prevents current leakage in the body. Stray electricity without proper grounding close to the surface electrodes could both be harmful to the person and cause inaccurate EMG readings from the BioRadio. A good placement of the ground electrode for this would be on a surface that is electrically inactive, yet close to the surface electrodes – like the elbow, with no muscle or highly active tissue. (2) For both types of electrodes, the skin was also wiped with alcohol and prep gel to ensure there is no excess moisture or oil that could tamper with the EMG readings. (3) As per this insight, the electrodes have been placed as per Figure 1 in Appendix A.

Upon pairing the BioRadio to the computer, the device was configured at Channel 1, with a sample rate of 2 kHz with no other channels and sensors. This sampling rate was determined by Nyquist's theorem, which states that any periodic signal (such as the one attained by the BioRadio) must have a sampling rate that is twice the upper bound frequency of the signal itself in order to ensure there is no loss of information without generating more samples than needed. (4) According to the user manual for BioCapture software, this upper bound frequency seems to be approximately 1000 Hz (exactly 960 samples per second), meaning the sampling rate as per Nyquist's theorem should be 2 kHz. (5)

EMG readings were recorded for approximately 15-30 second time intervals for two flexions. Once recorded, three sets of data were recorded for processing: two csv files containing raw and filtered EMG data, as well as the original bcrx data file from the BioCapture software. In MATLAB, the raw and filtered csv files can be visualized and compared.

The second half of the lab procedure removes the surface electrodes on the bicep and instead places them on the forearm (as shown in Figure 2 of Appendix A).

Instead of recording from the BioCapture software, the BioRadio is instead streaming the data to MATLAB directly using the provided MATLAB SDK package. MATLAB scripts were provided that utilized Arduino's compiler to capture flexion responses in fixed 30 second intervals. Using the BioRadio_Stream function, real-time connection with MATLAB and reading of EMG data from the BioRadio was confirmed.

Once the previous was confirmed, a circuit on an Arduino Uno was created to link a servo motor and a couple of LEDs to indicate whether peaks in EMG readings can activate the servo motor (shown in Figure 3 of

Appendix B). The two LEDs were connected in series at pin 13 on the Arduino board. The two LEDs are placed in series since keeping a singular LED in the circuit at the given voltage of the Arduino board could easily burn the component without the added resistance of the second LED in series. The servo motor is given 5V power and proper grounding and a connection to pin 9.

Once all is connected, the sample script arduino.ino given can be run with the port number and board set to that of the Arduino Uno used. This script checks every loop whether the servo motor has been given instructions to turn on through a parsed integer value from a serial input. If that state is turned on (1), the LEDs should turn on and the servo motor spins 90 degrees, otherwise, it should keep the LEDs and the servo motor off.

Finally, with the EMGdemo.m file provided, the code can be run in MATLAB to provide serial input to the Arduino depending on whether EMG data observations exceed 0V. Utilizing the arduino_Stream.m file provided, the threshold voltage parameter was tuned from 0 to 0.005V and the Arduino flag parameter was also set to 1. With these changes to the code, the servo motor was able to move when the fist was clenched.

Discussion

Two trials of EMG recordings were done for elbow flexion with electrodes on the bicep. However, upon transferring the data between machines, the files for the second trial were not properly exported, losing the csv files in the process. Unfortunately, data from only the first trial can be considered. All analysis on the raw and filtered csv files was done on MATLAB as per the script in Appendix B.

It becomes clear that the raw and processed EMG signals are very different from each other. Upon import and observing the BICEP section, it seems that the filtered and raw data seem to be noticeably different from each other. Both sets of data contain different ranges of values, with the filtered data in approximately [-0.2, 0.2] excluding outliers and the raw data being a factor of ten behind at approximately [0.01, 0.02]. The signal-to-noise ratio (SNR) was determined to be around -7.90 dB with a noise power of 5640 W. Figure 1 shows the spectrum plot.

Figure 1. Spectrum with the SNR for DC, fundamental frequency, and other harmonics

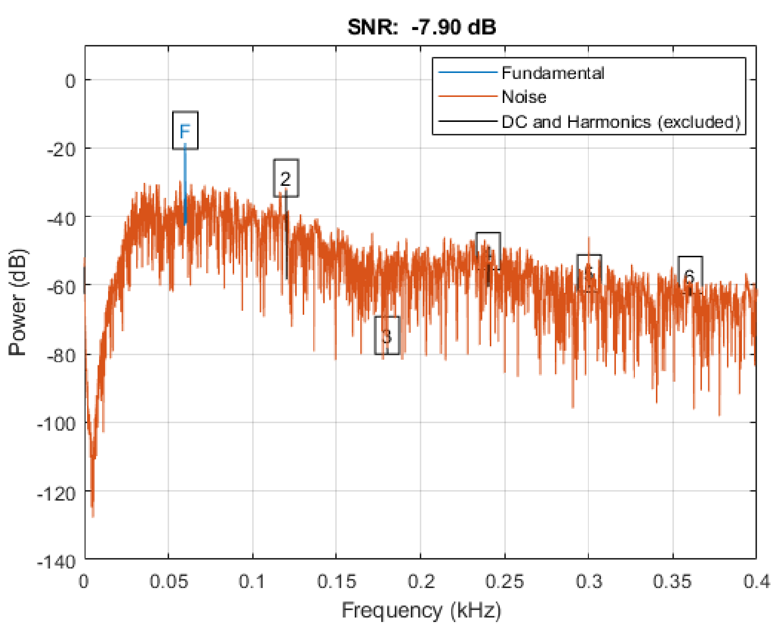

Sources of this much noise could stem from many different issues. The distance between the electrodes might have been too large, causing some cross-reading from other muscles. There could have also been some moisture still remaining on the skin just before applying the electrodes that could have created erroneous data. However, noise is always going to be present in data, no matter how precise the instrument is. Because the instrument is trying to continuously record data in discrete time, fluctuations are bound to occur.

The SNR being -7.90dB does create some limitations of our measurements as magnitudes of SNR readings below 15dB indicate contamination with high- and/or low-frequency noise, which leads to significantly erroneous observations. (6) Furthermore, the indication that the SNR is negative means that there is more noise than there is the signal, meaning that there is a lot of lost information within the signal.

Converting the raw EMG signal into the frequency domain and plotting it resulted in Figure 2.

Figure 2. FFT plot of the raw signal data in the real domain

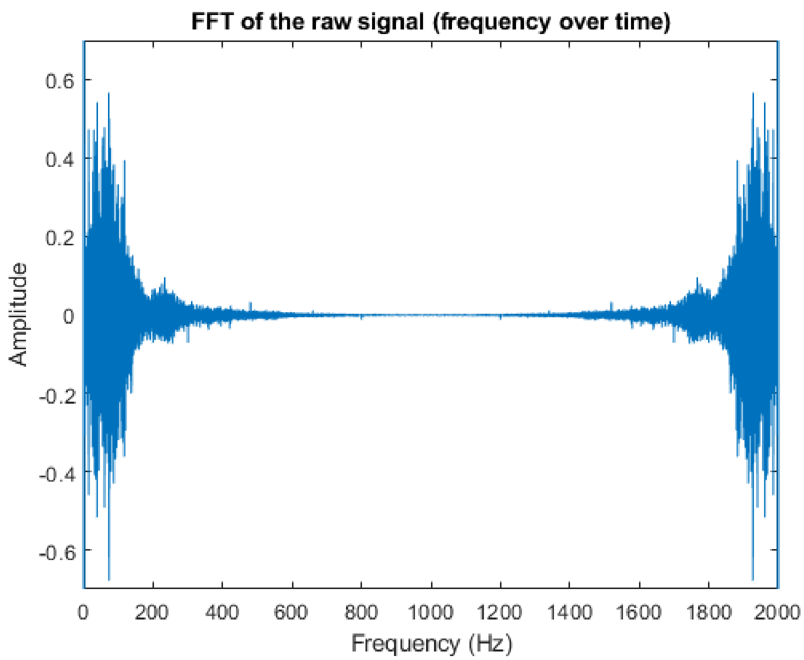

This Fast Fourier Transform (FFT) plot can help us identify the cut-off frequency for the 4th order butterworth band pass filter. Since it would not make sense for the data to be in the 1600 to 2000 Hz range when the max sampling frequency of the BioRadio was 1 kHz, the main part of the signal should rather be in the 0 to 200 Hz range, where the frequency had noticeable amplitude. 200 Hz onwards suddenly drops in amplitude and could easily be seen as the noise produced in the signal. Therefore, the passband should be somewhere from 0 to 200 Hz. After finetuning, the best cut-off frequencies were determined as 50 Hz and 185 Hz. The plot in Figure 3 shows the filtered signal against the time domain, as well as after removing the DC offset and performing a full-wave rectification.

Figure 3. The filtered signal against the time domain before and after DC offset removal and rectification

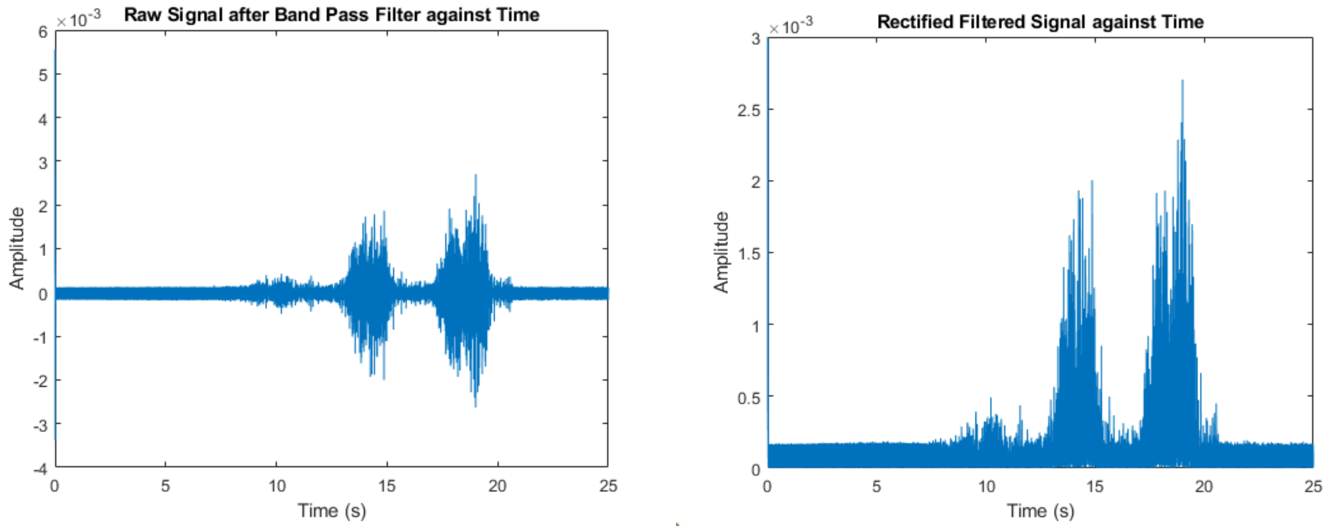

Something to note is what happens to the rectified signal after changing the cut-off frequencies (displayed in Appendix C). It seems that the larger the cut-off frequencies, the smaller the amplitudes and vice versa. This also seems to be the case with the SNR values. These can vary based on the site of the electrodes since different muscles can result in different electric activities. For example, electrodes placed on the thighs would produce require a higher passband than the biceps, as they have an average EMG reading higher. (7) Thus this relationship would be skewed right a bit. The envelope function in MATLAB was used in order to create upper and lower envelope slopes for the filtered signal, as shown in Figure 4. After trial and error, the window size was chosen to be 300. When the window size is too large, the envelopes become too simple and further from the general size of the signal. Making the window size too small caused the envelopes to become just as busy and noisy as the signal, which would not be helpful. With these factors in consideration, the window size was met at the midpoint, close to the upper cut-off frequency of the filter.

Figure 4. Filtered signal with lower and upper envelopes

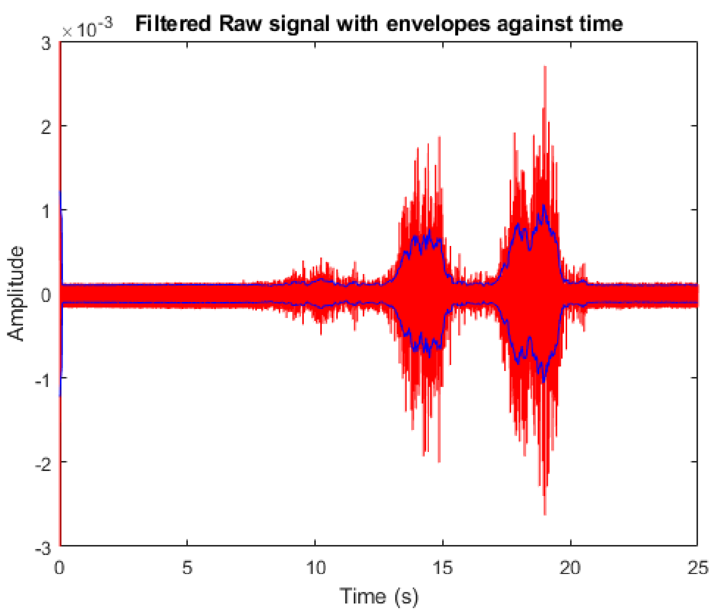

Using the envelopes, the onset of muscle activation for the first pulse was at around 13s, with an offset at around 15. The onset is useful for EMG analysis as it states where pulses and sudden activities in the muscle happen, meaning that any noise or silence out of that window can be disregarded, leading to more accurate observations when only considering data within this time. Using the cumtrapz function in MATLAB, the integrated EMG for the signal can be calculated, which was also plotted (seen in Appendix D). The trapz function was also utilized to convert it into a scalar number, which was calculated to be around -2.02e-07. Finally, we can perform the EMG signal normalization. By observing the graph, the maximum voluntary contraction (MVC) magnitude is roughly 2.55mV. Utilizing the equation provided in the lab manual, the normalized EMG was created and plotted. Figure 5 shows the comparison between the normalized signal. When compared to the original signal, the amplitude is much larger and the non-active sections seem to be much more stable at resting potential (as opposed to the much busier resting windows in the original signal). Normalization is necessary because the EMG signal is now put against a reference value to ensure that there is a clear distinction between active and non-active windows.

Figure 5. Normalized signal

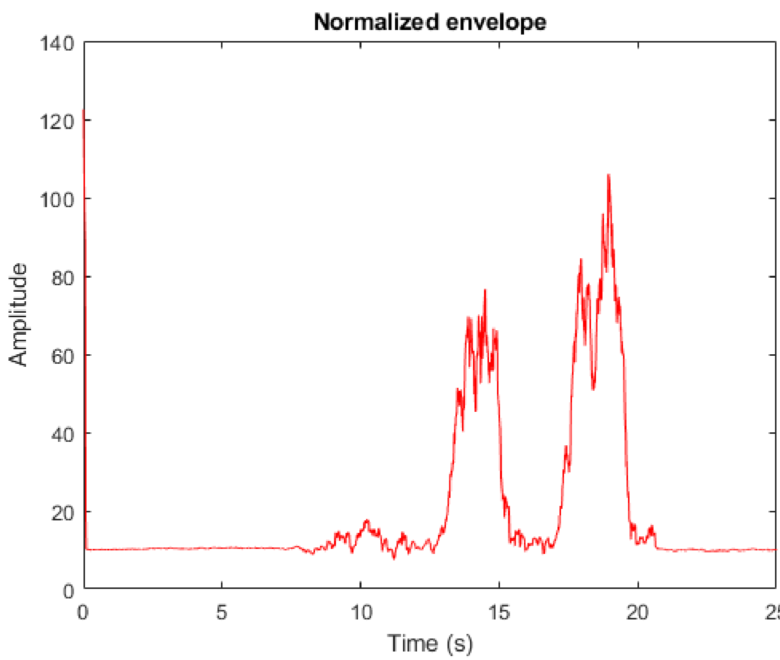

The same techniques utilized above can also be used to process the data created in the second half of the experiment (outlined in the code in Appendix E). Figure 6 shows the pre-processed and processed data. When comparing the processed results of this signal with that in Figure 5, it becomes immediately clear that there was much more activity (larger amplitude spikes), which is most likely since clenching of the fist, especially in this lab, resulted in much stronger activity than simply flexing the elbow. As such, EMG readings on the forearm are going to read much higher EMG values than those on the bicep. There also seemed to be much more fluctuating noise in the signal, which meant that the passband had to be lower in order to omit higher noise frequencies.

Figure 6. Pre-processed and processed signal in the second half of the experiment

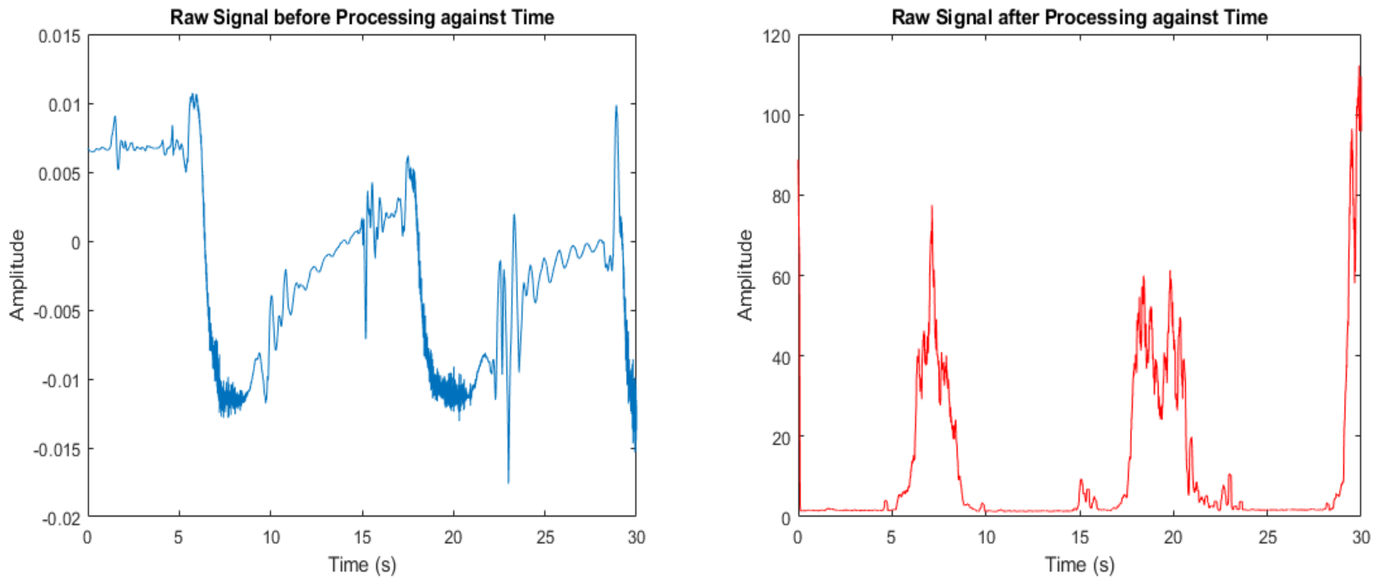

Conclusion

In this lab, EMG readings were recorded from the biceps and the forearms in two different experiments. The first tested EMG values in the biceps through elbow flexions and the second tested EMG values in the forearms with fist clenches. Utilizing MATLAB's software, we were able to employ bandpass filters and RMS envelopes to properly filter noisy observations in data to provide a cleaner, detailed curve to view patterns and pulses of interest. The code provided for this lab was utilized to make a servo motor run properly when the fist was clenched.

Specifically for the second experiment, it is worth noting that this type of control functionality is especially useful in the field of active prosthetics. EMG and EEG signal interpretation, especially in the brain, can be used to translate motor commands to the prosthetic that would normally go to a limb connected to the central nervous system. In practice, high levels of focus and concentration are required to properly translate such EMG/EEG signals to movement, especially when data could become complicated and noisy with the number of daily distractions from environmental factors and non-locomotion-related brain activity. (8) This highlights the requirement to understand proper filtering techniques such as the ones employed in this lab. Without proper filtration, there is no way for the prosthetic to know which EMG/EEG signals belong to which function. This also becomes a challenge when considering non-invasive solutions, such as utilizing surface electrodes near the amputation and pattern recognition AI to create a possible solution, the next issue being that the pattern detection is not always 100% accurate and that many – as much as 16 – electrodes are needed, contrary to the 3 we used in this lab. (9)

Besides the biomedical field, another notable field that utilized EMG signals is game creation and programming, specifically in creating bio-signal-based interfaces that can utilize basic EMG data from skin response, motor control, and eye movement to translate into actions within a virtual environment. Similarly, it can be used in vocal signal processing fields because speech can be recognized by muscle activity, specifically in the face and jaw, which can be very useful in extended fields that might want to observe how speech and facial movement are connected such as the field of robotics. (10)

References

1. Merlo A, Bò MC, Campanini I. Electrode size and placement for surface EMG bipolar detection from the brachioradialis muscle: A scoping review. Sensors. 2021;21(21):7322.
2. Tankisi H, Burke D, Cui L, de Carvalho M, Kuwabara S, Nandedkar SD, et al. Standards of instrumentation of EMG. Clinical Neurophysiology. 2020;131(1):243–58.
3. Jamal MZ. Signal Acquisition Using Surface EMG and Circuit Design Considerations for Robotic Prosthesis. In: Naik GR, editor. Computational Intelligence in Electromyography Analysis - A Perspective on Current Applications and Future Challenges [Internet]. London: IntechOpen; 2012 [cited 2022 Feb 06]. Available from: https://www.intechopen.com/chapters/40131 doi: 10.5772/52556
4. Colarusso P, Kidder LH, Levin IW, Neil Lewis E. Raman and infrared microspectroscopy. Encyclopedia of Spectroscopy and Spectrometry. 1999;:1945–54.
5. BioCapture User Guide. Cleveland: Cleveland Medical Devices Inc.; 2011.
6. Li J, Wang P, Huang HJ. Dry epidermal electrodes can provide long-term high fidelity electromyography for limited dynamic lower limb movements. Sensors. 2020;20(17):4848.
7. Muyor JM, Martín-Fuentes I, Rodríguez-Ridao D, Antequera-Vique JA. Electromyographic activity in the gluteus medius, gluteus maximus, biceps femoris, vastus lateralis, vastus medialis and rectus femoris during the monopodal squat, forward lunge and lateral step-up exercises. PLOS ONE. 2020;15(4).
8. Tucker MR, Olivier J, Pagel A, Bleuler H, Bouri M, Lambercy O, et al. Control Strategies for active lower extremity prosthetics and orthotics: A Review. Journal of NeuroEngineering and Rehabilitation. 2015;12(1):1.
9. Ciancio AL, Cordella F, Barone R, Romeo RA, Bellingegni AD, Sacchetti R, et al. Control of prosthetic hands via the peripheral nervous system. Frontiers in Neuroscience. 2016;10.
10. Reaz MB, Hussain MS, Mohd-Yasin F. Techniques of EMG signal analysis: Detection, processing, classification and applications. Biological Procedures Online. 2006;8(1):11–35.

Appendix A

Images for electrode placements and circuit construction of the experiment

Figure 1. Electrode Placement on the Biceps for Elbow Flexion

Figure 2. Electrode Placement on the Forearms for Elbow Flexion

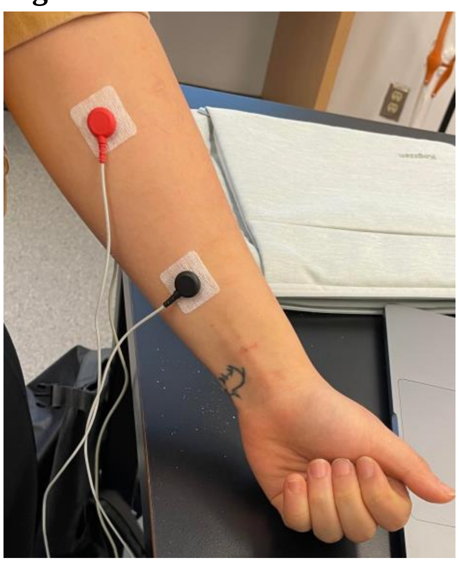

Figure 3. Connection of the servo motor and LEDs to the Arduino Uno.

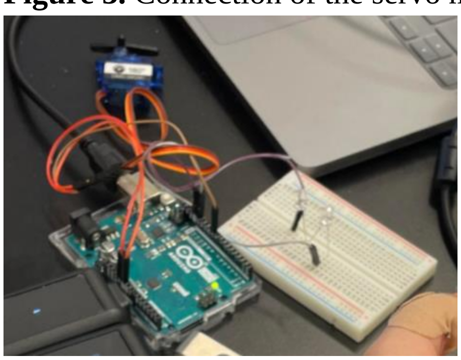

Appendix B

Code for Part C analysis

The code for Part C can be found through the following GitHub link:
https://github.com/HyprValent/bmeg_321/blob/main/lab_2/lab2_partc.m

Appendix C

Rectified signals at differing cut-off frequencies

Rectified signal at 200Hz to 500Hz bandpass:

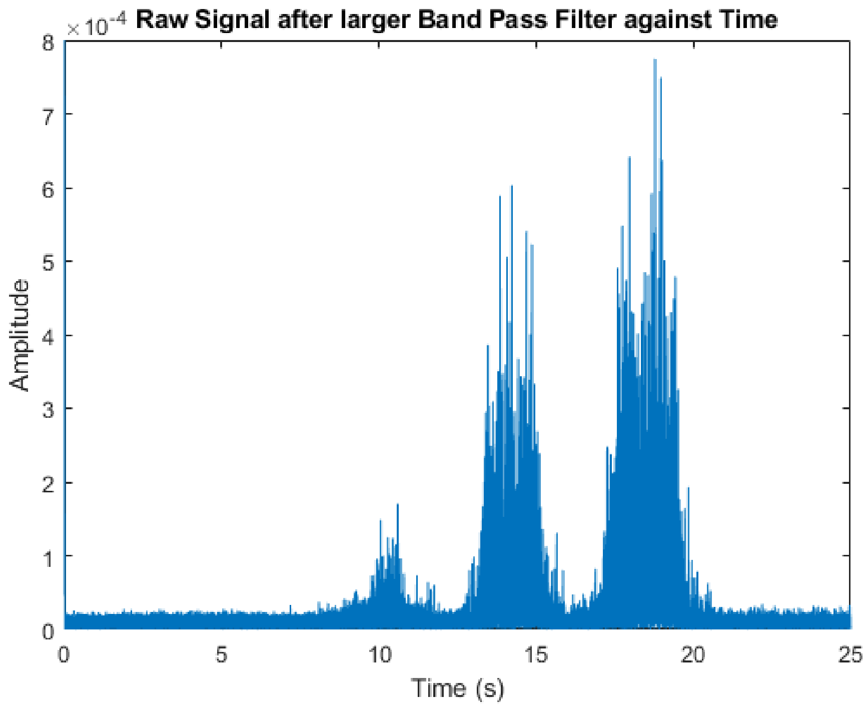

Rectified signal at 10Hz to 100Hz bandpass:

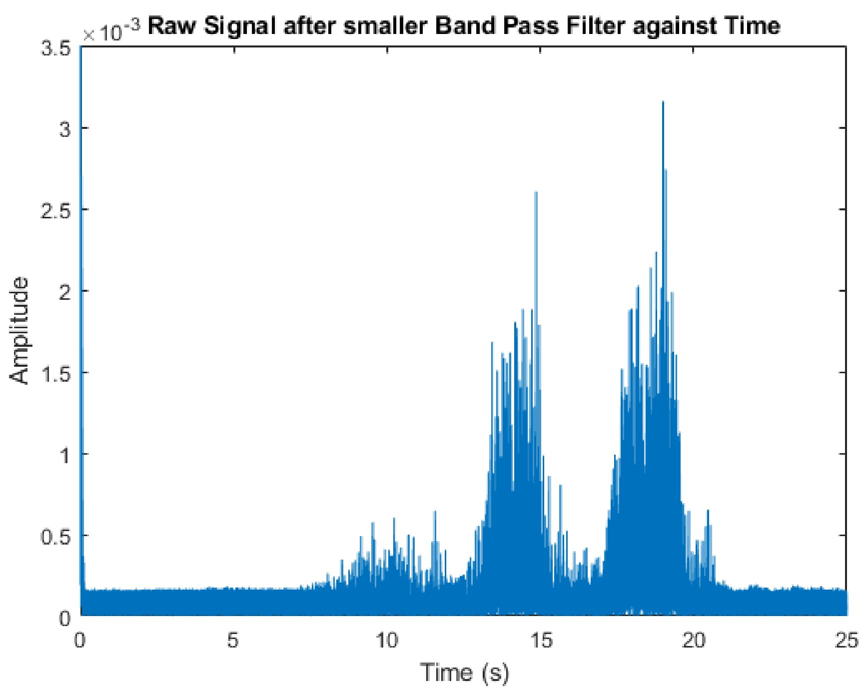

Appendix D

Integral of filtered signal

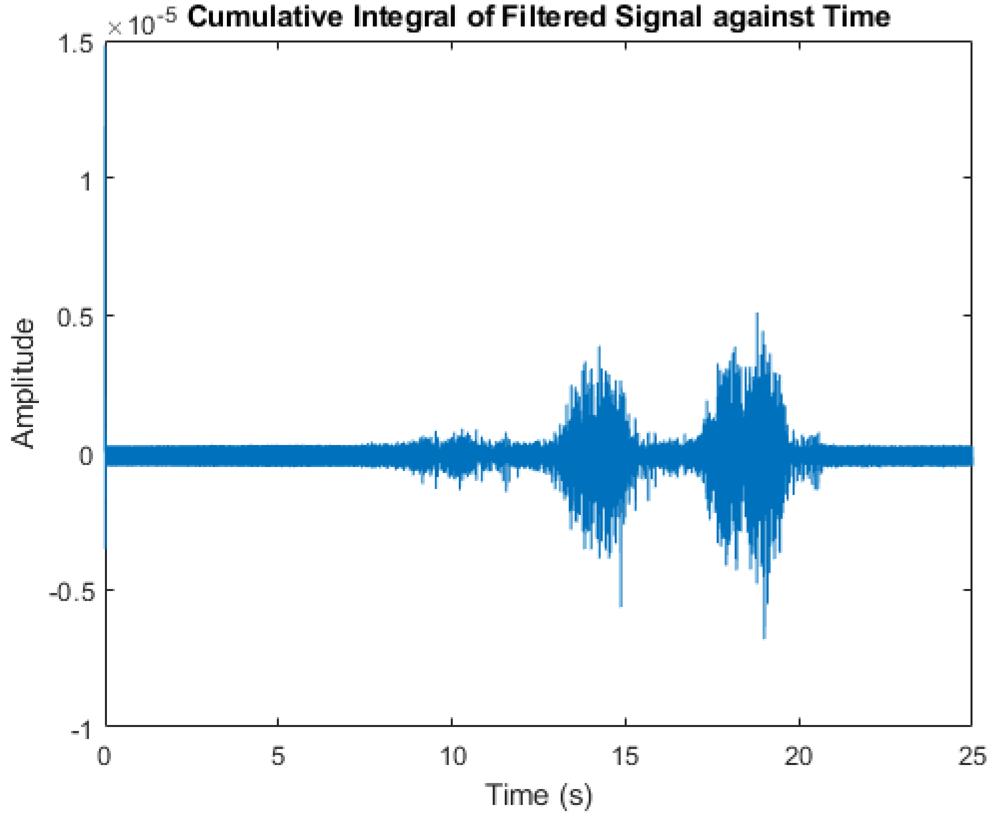

Appendix E

Code for signal processing in Part D analysis

The code for Part C can be found through the following GitHub link:
https://github.com/HyprValent/bmeg_321/blob/main/lab_2/lab2_partd.m